We are IntechOpen, the world's leading publisher of Open Access books Built by scientists, for scientists

4,800
Open access books available

122,000
International authors and editors

135M
Downloads

Our authors are among the

154
Countries delivered to

TOP 1%
most cited scientists

12.2%
Contributors from top 500 universities

WEB OF SCIENCE™

Selection of our books indexed in the Book Citation Index in Web of Science™ Core Collection (BKCI)

Interested in publishing with us?
Contact book.department@intechopen.com

Numbers displayed above are based on latest data collected.
For more information visit www.intechopen.com

Chapter 4

Experimental and Simulated EMG Responses in the Study of the Human Spinal Cord

Rinaldo André Mezzarane, Leonardo Abdala Elias,
Fernando Henrique Magalhães,
Vitor Martins Chaud and André Fabio Kohn

Additional information is available at the end of the chapter

http://dx.doi.org/10.5772/54870

1. Introduction

Advances in the study of human spinal cord neurophysiology have been strongly based on the analysis of the electrical activity of muscles (electromyogram - EMG). The EMG measured over the skin reflects the general behavior of motor units (MUs) and hence of spinal motoneurons (MNs). It can be used, for instance, to infer changes in the behavior of neuronal circuits within the spinal cord during the performance of a motor task or in response to peripheral and/or descending inputs.

In the beginning of the 20th century, Paul Hoffmann introduced a non-invasive technique – the H-reflex – that helped to pave the way for subsequent investigations into the mechanisms of stretch reflex regulation [1]. The neuronal organization of the spinal cord is now better understood thanks to studies of reflex modulation in response to different conditionings and motor contexts, e.g., electrical or mechanical stimulation of sensory afferent pathways, magnetic or electric activation of descending tracts (DTs), passive movement of limbs and joints, voluntary isometric contractions and performance of motor tasks.

Reflexes play a fundamental functional role in motor control, as they are involved in the coordination of voluntary movements and maintenance of postural stability. This justifies the high contingent of fibers from peripheral (cutaneous, muscle and joint afferents), segmental (propriospinal interneurons), and supra-segmental (descending tracts) origins that synapse on different spinal cord elements (synaptic terminals, interneurons and MNs). This also highlights the important integrative function of the spinal cord, contrasting with the naive

notion that it is only a relay station, or a pathway that simply transfers information from the brain to the muscle fibers.

Despite the relative limitations of non-invasive techniques employed in humans, it is currently possible to establish a parallel between the findings from animal preparations (such as cat) and experiments in humans (e.g., [2, 3]). In addition to the use of animal models as aids for understanding human data, another source of information comes from new multi-scale computer simulators of neuronal circuitry and muscle control [4, 5]. Moreover, with the development of these simulators, supported by anatomical and biophysical data from animal experiments, it is also possible to reinforce hypotheses formulated to explain experimental results obtained from humans (e.g., [5]).

The aim of the present chapter is to provide some conceptual and methodological background for researchers and clinicians who intend to use EMG to study human spinal cord neurophysiology. Here we will discuss different methods frequently used in the study of human neurophysiology based on surface EMG. These will be illustrated by results from both experimental studies and simulations performed in a multi-scale model of the spinal cord and leg muscles. Additionally, a brief account will be given of some processing techniques of surface EMG that are used to quantify spinal cord excitability and effects of inhibitory pathways. The methods explored in the chapter have been used in both healthy subjects and patients with a variety of neuromuscular disorders.

2. Brief review and basic methodological considerations

This brief review presents a few basic concepts related to electrical muscle activity recorded with electrodes over the skin. Methodological aspects that might influence the interpretation of experimental results are discussed. Further details concerning these basic aspects can be found elsewhere [6, 7].

2.1. Some important definitions

In the preceding section we have referred to EMG as the electrical muscle activity recorded with surface electrodes. This electrical activity is the result of the depolarization of a number of muscle fibers. A group of muscle fibers innervated by the same spinal cord MN is called a muscle unit while the MN and the muscle unit it innervates is the motor unit (MU). During voluntary muscle activation, the number of recruited muscle fibers contributing to the EMG depends on the net excitatory drive from the brain and peripheral sensory afferents arriving onto the spinal MNs. During a mild voluntary contraction only a small fraction of MUs is recruited. As the excitatory command is increased, two distinct mechanisms take place: the MUs previously recruited increase their firing rate (rate coding) and new MUs with higher firing threshold are recruited (population coding). These basics may be found in many references, such as [8].

The activity of a single MU is easily recorded with needle electrodes inserted into the muscle (the most common is the concentric needle electrode). However, during low-intensity con-

http://dx.doi.org/10.5772/54870

traction, surface electrodes can also record activity of superficial MUs [9] as can be seen in the upper trace in Figure 1. For increased levels of voluntary contraction additional MUs are recruited (see middle trace in Figure 1). For high-intensity contraction the EMG recording tends to show a filled random pattern due to the superposition of a greater number of MU action potentials (MUAPs) known as interference pattern (bottom trace in Figure 1). Thus, the interference pattern of the EMG is associated with the asynchronous firing of different MUs. When the conditioning of an interference pattern EMG is used to infer spinal cord processes, the experimental control of the level of activity is crucial. When the strength of descending commands changes, different populations of MNs and interneurons (INs) are recruited, leading to different conditioned EMG responses.

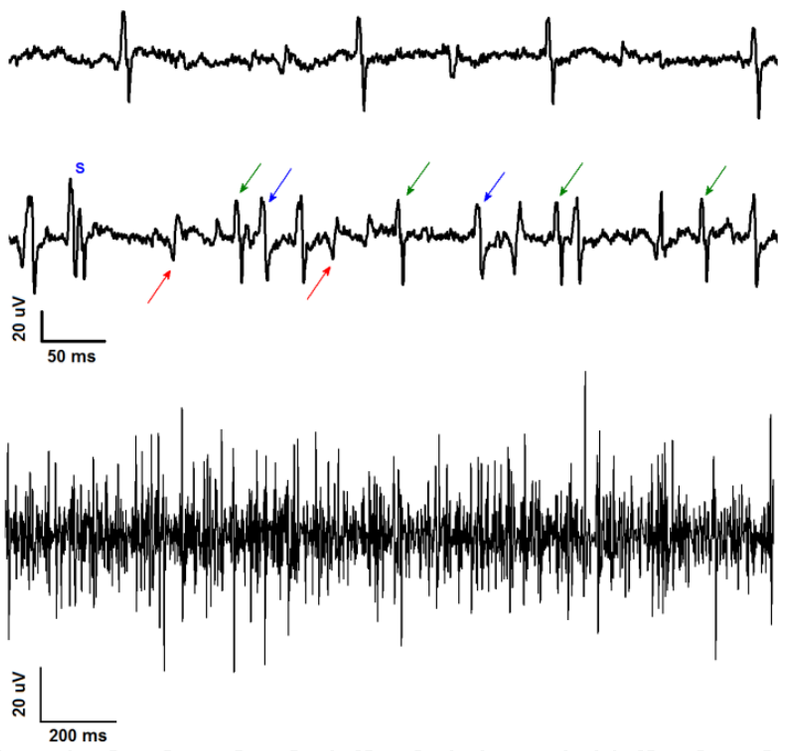

Figure 1. Surface EMG recordings from soleus (SO) muscle during a weak contraction (unpublished data). Upper panel: EMG recording during a very weak contraction in which only one MU is recruited. Middle panel: when the subject was told to slightly increase the voluntary contraction, the MU previously recruited increased its firing rate (see the green arrows) and other MUs with different firing rates were recruited (red and blue arrows). The letter "S" indicates a sum of at least two distinct MUAPs. Lower panel: Interference pattern of EMG.

2.2. Acquisition

Some technical aspects need to be considered for an accurate recording of the EMG signal. Here we are going to briefly discuss filtering, sampling rate and electrode positioning.

The spectral composition of a signal has implications on the choice of the band-pass filter cutoff frequencies used before the analog-to-digital conversion as well as for the selection of a suitable

sampling frequency (SF). Figure 2 shows the power spectrum of an EMG recorded with surface (upper panel) and needle (lower panel) electrodes during a sustained contraction. It is interesting to note the dramatic difference in the spectra of both recordings (note the different calibrations of the abscissa). For the surface EMG, band-pass filter cutoff frequencies from 10Hz to 500Hz would be appropriate and a SF of at least 1kHz would be used; however, in the second example, the 500Hz cutoff frequency (see the red area in the lower panel of Figure 2) would be clearly inappropriate due to the significant contributions of high-frequency spectral components of the signal. Therefore, when using needle EMG, the high-frequency cutoff should be higher, e.g., 5kHz-10kHz and sampling done at 20kHz-40kHz.

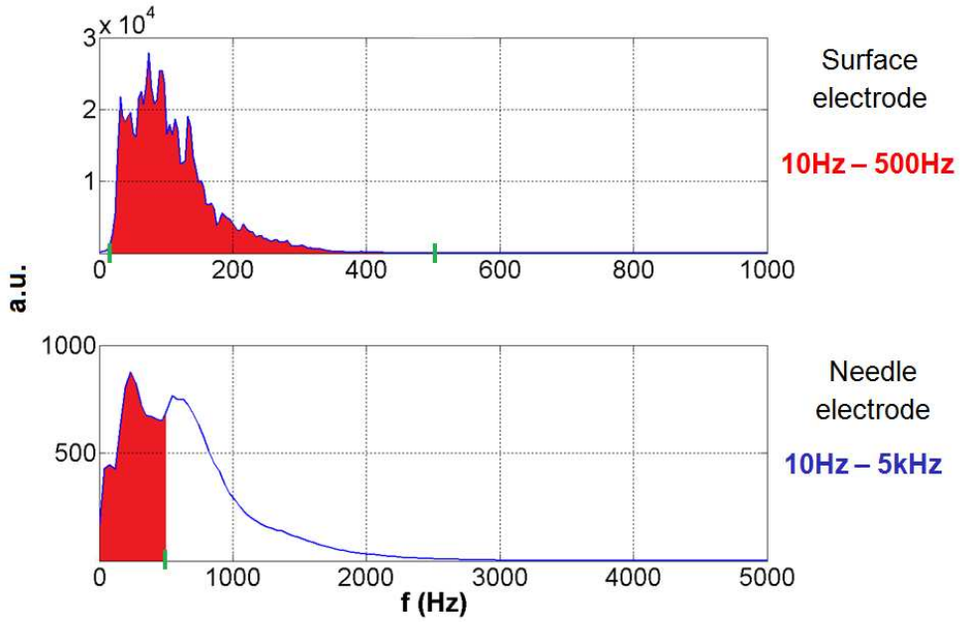

Figure 2. Power spectra of EMG signals from the SO muscle recorded with surface (upper panel) and needle (lower panel) electrodes (unpublished data). They show the frequency content (in Hz) of each signal. The green marks in the abscissa (small vertical lines) comprise the frequencies of the band-pass filter used for surface EMG. The corresponding frequency ranges are indicated in red (upper panel) and in blue (lower panel) for surface and needle recordings, respectively. It is clear in the lower panel that if we used the same frequency range of surface EMG for needle EMG a considerable amount of information would be lost (see the red area delimited by the green marks).

The choice of a suitable frequency range for the band-pass filter to be applied to the surface EMG signal needs to be done with caution according to the objectives of the study. A wrong choice of filter parameters may cause information loss and misleading interpretations of the results. For instance, if the focus is to investigate slow variations of the surface EMG signal during stepping or gait (e.g., EMG envelope), a frequency band of 10-300Hz could be adequate [10]. However, using the same recording technique to evaluate reflex components (e.g., H-reflex), the high cutoff frequency should be raised to 1kHz (with a SF of at least 2kHz) for better reproduction of the phasic EMG signal generated [10].

Generally, in surface EMG, the electrodes are located on the skin above the belly of the muscle of interest, in a region between the tendon and the innervation zone [11]. The electric currents

http://dx.doi.org/10.5772/54870

generated by depolarization of the muscle fibers travel through the connective tissues, fat, vessels, skin (all of which comprises the volume conductor), reaching the region underneath the electrodes. The volume conductor has the property of a low-pass filter [12] and the signals reach the electrodes placed over the skin with a slower time course and decreased amplitude. On the other hand, a needle electrode is much closer to the source of the electrical activity than a surface electrode and hence it does not suffer the low-pass filtering and amplitude attenuation caused by volume conduction [6, 12]. This explains why the needle EMG signals have better signal-to-noise ratios and why their power spectra have components at higher frequencies (see the lower panel in Figure 2).

The main advantage of invasive techniques such as needle or wire EMG is its high selectivity (one or very few MUs can be recorded with a high signal-to-noise ratio). Conversely, this may be a disadvantage when the purpose is to evaluate a larger number of MUs to obtain a more comprehensive view of muscle activation. In this case, surface EMG is more indicated. The main shortcomings of surface EMG are that (1) not all muscles are superficial and (2) the possibility of interference from nearby muscles' electrical activities on the EMG signal recorded from the desired muscle. These recorded interferences are attenuated or perhaps distorted versions of the electrical activities from the nearby muscles and are known as crosstalk [13, 14]. The crosstalk effect can sometimes be minimized by a careful placement of the electrodes.

The distance between electrodes is a key factor to increase or decrease the relative selectivity of the EMG recording. Figure 3 shows an example in which the EMG activity is recorded with an array of three electrodes. When the potential difference is calculated between the more distant pair of electrodes (E1 – E3) the recording is less selective than when the electrodes are closer to each other (E1 – E2).

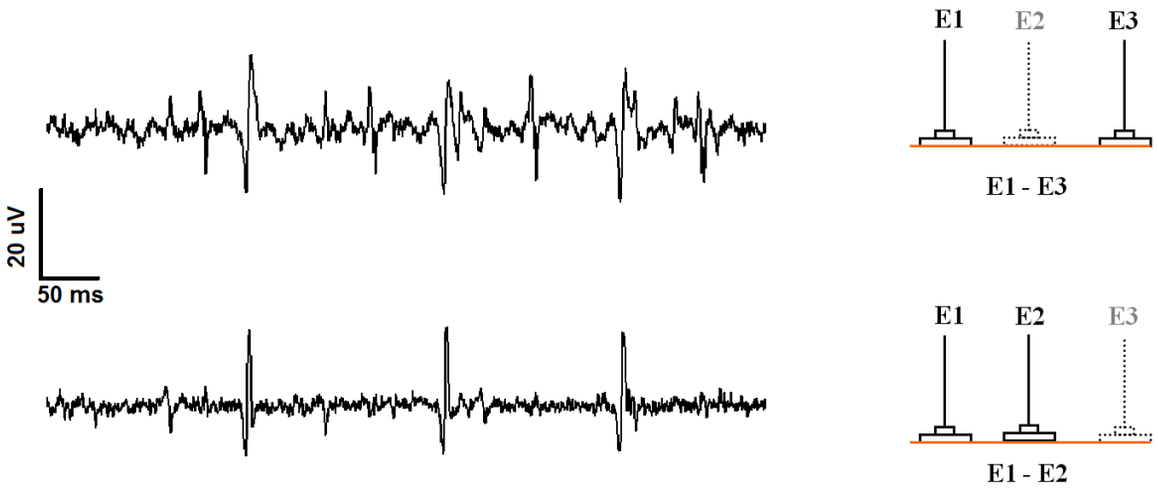

Figure 3. Surface EMG showing the effect of the distance between electrodes (unpublished data). Upper panel: EMG recorded with a distance of 2.5cm between electrodes (E1-E3). The lower panel shows the same recording with inter-electrode distance of 1cm (E1-E2).

3. Conditioning of the constant ("asynchronous") muscle activity

The EMG interference pattern is useful to help understanding the conditioning effects coming from a variety of sources. These conditionings fundamentally act on the modulation of muscle activity and are context-dependent [15]. Therefore, it is possible to study the effects of a variety of inhibitory and excitatory pathways on MNs by means of EMG signal conditioning, and hence extract information on spinal cord neurophysiology.

The voluntary activity of the SO muscle (sustained low-level isometric contraction) can be modulated by the activation of the primary (Ia) afferents from the antagonist muscle spindles [15, 16]. The diagram depicted in Figure 4 shows surface transcutaneous electrical stimulation (1ms rectangular pulse) applied to the common peroneal nerve (CPN) that supplies the tibialis anterior (TA) muscle. The conditioning stimulus substantially reduces the SO muscle activity via reciprocal inhibition (RI) [16]. A typical example of the resulting EMG signals is shown in Figure 5.

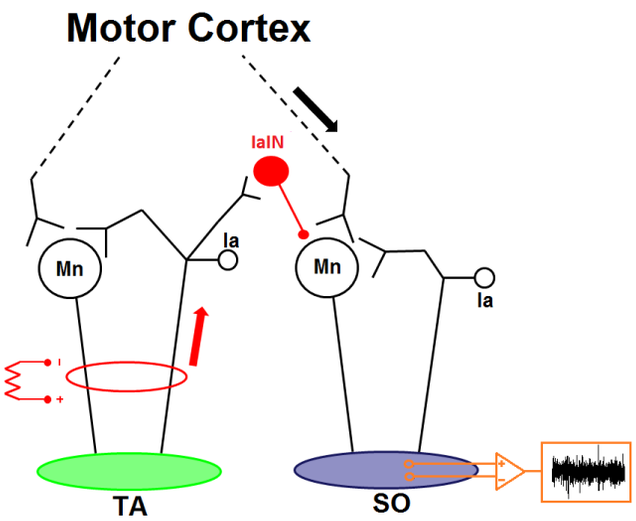

Figure 4. Schematic showing the pathway of reciprocal inhibition (RI). The black arrow indicates the descending drive from the motor cortex to the SO muscle that generates the interference pattern shown in the oscilloscope (small rectangle in orange color). The EMG activity can be conditioned by an electrical stimulus applied to the nerve that supplies the antagonist muscle (TA). The action potentials in the Ia afferents (red arrow) activate the inhibitory Ia IN (IaIN) that generates an inhibitory post-synaptic potential (IPSP) in the membrane of the MN. Hence, after the conditioning electrical stimulus, some MNs will stop firing and the EMG interference pattern will show a transitory decrease in the amplitude (see also Figure 5).

Looking at one or a few sweeps of conditioned-EMG signals (left panel of Figure 5), it is not possible to determine if the inhibition is present. Note that the low voluntary muscle activity produced a very sparse MU firing in the recordings (upper traces) shown on the left panel of Figure 5. When the sweeps (a total of 50) are superimposed (lowermost signal at the left panel of Figure 5), the inhibition becomes clear (see the red horizontal bar below). Thus, several tenths (or even hundreds) of stimuli are necessary to allow the detection/quantification of the

http://dx.doi.org/10.5772/54870

effect of RI on the SO MNs [1]. However, to quantify the amount of inhibition, additional signal processing of the EMG signal is needed: (1) subtraction of the DC level, (2) computation of the absolute value of each EMG sample, also called EMG rectification, (3) computation of the ensemble average of the several rectified conditioned-EMG signals (or sweeps). The number of sweeps to be averaged depends on the strength of the conditioning effect and the level of voluntary muscle contraction [16]. These procedures will be illustrated based on the superimposed sweeps shown at the right uppermost panel of Figure 5. The results of step (2) above are shown in the middle panel at the right of Figure 5. The bottommost trace of the right panel of Figure 5 is the ensemble average of the traces displayed just above it (step 3).

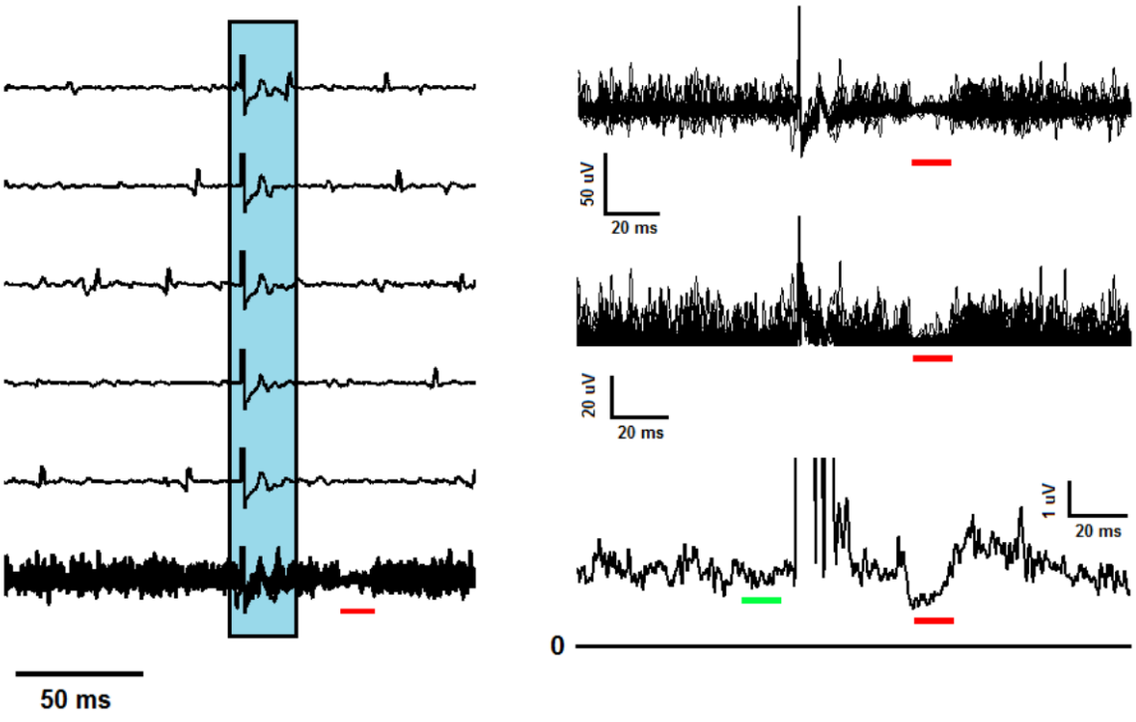

Figure 5. Left panel: EMG recordings of the SO showing the muscle activity before and after the delivery of an electrical stimulus to the CPN nerve (unpublished data). The traces show sparse MU firings. The rectangle in blue encompasses the stimulus artifact followed by a crosstalked activity from the antagonist (TA) muscle. An interesting observation is that the inhibition is not quite clear by the examination of a single recording. The bottom trace shows all the 50 recordings superimposed. A clear reduction in muscle activity ~40ms after the electrical stimulation is indicated by a red bar. Right panel: same traces superimposed (upper trace). All the EMG recordings were rectified (superimposed traces in the middle) and averaged (bottom trace). The red bar indicates the reduction in muscle activity due to RI induced by the procedure depicted in the schematic of Figure 4.

The inhibitory period indicated by the red bar under the averaged trace of Figure 5 can then be quantified either by the peak (lowest point of the recording), the mean or the RMS [7] and normalized with respect to a similar computation of the pre-stimulus period (green bar). In an alternative approach, RMS values in each sweep at the right-top corresponding to the time windows defined by the green (control) and red (inhibited) bars are computed and averaged. This yields a mean RMS value in the control period and a mean RMS value in the time interval

associated with the effect of the RI. To allow comparisons between subjects one may adopt the ratio of the latter to the former as an index of the level of RI.

Besides changing the excitability of MNs, pathways converging to the spinal cord may also affect the excitability of several spinal cord elements by acting on presynaptic terminals (e.g., the Ia-MN synapse). Presynaptic effects will be discussed later.

4. Conditioning of the evoked phasic ("synchronous") muscle activity

So far, we have discussed the case of asynchronous voluntary activity of MUs that generates the EMG interference pattern. Another way to assess spinal cord processes is by means of reflex-generated compound muscle action potentials (CMAP).

A variety of reflexes (stretch reflex, cutaneous reflex, H-reflex, etc) has been studied at rest, during locomotion and during the performance of a number of motor tasks in an attempt to better understand how the central nervous system (CNS) integrates the descending signals with those coming from the periphery [1]. Ascending signals from the periphery are incorporated into motor plans in order to continuously update the CNS and generate suitable commands to muscles that will work in concert to produce a functionally relevant motor output. At the spinal cord level, the afferent influx coming from muscles, joints and skin help to sculpt motor behavior by playing a significant role in the modulation of the excitability of different reflex pathways [1].

The stretch reflex pathway is one of special interest and will be the focus of this topic. The excitability of this pathway (or parts of it) can be assessed by means of either electrical stimulation of peripheral nerve (H-reflex, F-wave and V-wave) or mechanical stimulation of the tendon (T-reflex). In what follows we will discuss the methodology of these techniques as well as their modulation in response to a variety of conditionings.

4.1. The H-reflex

The H-reflex was first described in 1918 by Paul Hoffmann [17] and is the electrical homologous of the stretch reflex. It is elicited by a transcutaneous electrical stimulation (rectangular pulse with 1ms duration) applied to a mixed nerve that synchronously activates afferent fibers from muscle spindles (see the arrow showing the orthodromic sensory activation in Figure 6). The evoked afferent volley generates excitatory post-synaptic potentials (EPSPs) in α-MNs (hereafter referred to as MNs) that may fire action potentials if they surpass the firing threshold. These EPSPs seem to be generated mainly by the monosynaptic Ia-MN excitatory pathway but they are also influenced by oligosynaptic pathways [18]. The action potentials originating from the MNs lead to the generation of a CMAP recorded with surface EMG electrodes at the homonymous muscle. The evoked CMAP is termed H-reflex and is different from the interference pattern of EMG described in the preceding text (see sections 2 and 3), which is characterized by the asynchronous firing of MUs. The technique of H-reflex has been widely used to assess the ex-

http://dx.doi.org/10.5772/54870

citability of the stretch reflex pathway and infer spinal cord mechanisms contributing towards motor control [1, 19]. In the lower limbs, the SO muscle has often been used because its electrically-elicited reflex response is relatively easy to obtain.The muscle afferents of group I (Ia and Ib) and II are also depicted in the schematic of Figure 6. However, for low intensity stimulation, group I muscle afferents (mainly Ia) are primarily activated [20].

The presence of a stable M-wave (direct motor response, see below) is desired in most studies to assure (by indirect means) a constant stimulation (see the arrow showing the orthodromic motor activation in Figure 6). Thus, any changes in H-reflex amplitude would be related to neurophysiological factors and not to alterations in stimulus efficacy, which would change the M-wave as well [21].

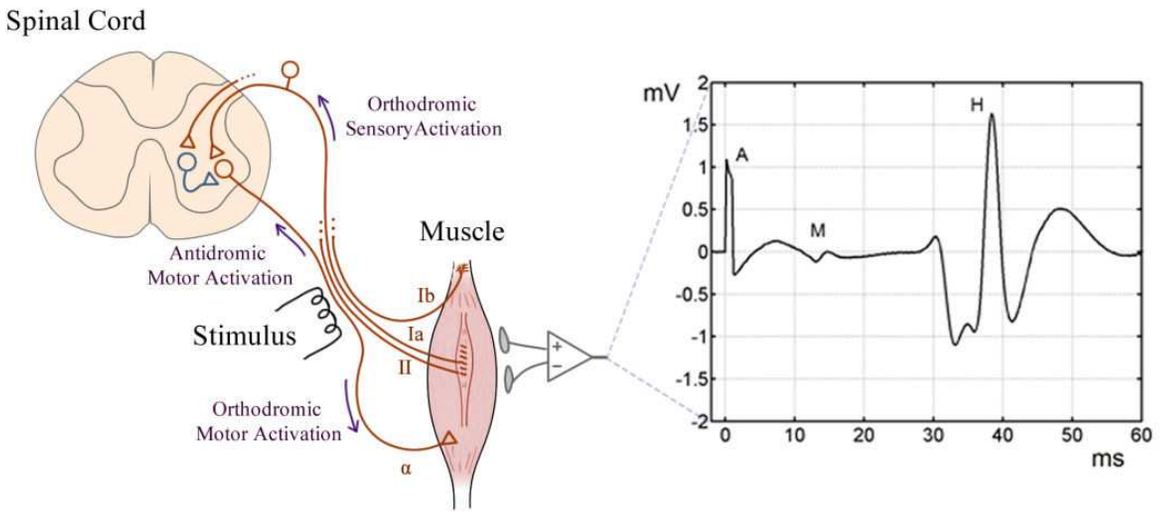

Figure 6. Schematic of the stretch reflex pathway and the mixed nerve stimulation that generates orthodromic and antidromic nerve activity (only the monosynaptic pathway from the Ia is shown). EMG trace showing an H-reflex and M-wave elicited by a transcutaneous electrical stimulus (1ms duration) applied through electrodes located over the skin at the popliteal fossa. The stimulus activates Ia afferent and motor axons from the mixed nerve (PTN) that supplies the SO muscle. The resulting H-reflex and M-wave are recorded with surface electrodes (see the schematic on the left). **A**: Stimulus artifact indicating when the stimulus was delivered; **M**: M-wave; **H**: H-reflex.

4.1.1. Recruitment order of reflexively activated motoneurons

With the increase of the stimulus intensity, a larger number of Ia afferents are activated leading to reflex recruitment of more MNs. The MNs in the spinal cord are synaptically recruited according to the size principle [22], i.e., the small size MUs (with low threshold for synaptic input) are recruited first. Therefore, H-reflexes of low amplitude reflect the activation of small MUs (see Figure 7). Higher amplitudes of H-reflex correspond to the activation of intermediated sized MUs along with the small ones. The increment in H-reflex amplitude reaches a limit that is not only related to the number of MNs within the pool, but also to the phenomenon of "annihilation", i.e., action potentials in the efferent axon generated reflexively collide with the

antidromic volley due to the firing of the distal part of the efferent axon by the electrical stimulus (Figure 8). Therefore, those motor axons that were activated by the transcutaneous electrical stimulation generate antidromic spikes (shown in Figure 6 as the "antidromic motor activation") that prevent the action potentials of reflex origin from reaching the muscle (see Figure 8). As the axonal conduction velocity of efferents is lower than the afferents, there is enough time for the collision to take place in the efferent axons. The action potentials generated in the efferent axons also propagate toward the muscle (orthodromic motor activation in Figure 6 and red arrows in Figure 8) and will generate a shorter latency response (M-wave). The stimulus intensity that generates the lowest amplitude M-wave is termed motor threshold (MT). The direct motor response (M-wave) increases monotonically with stimulus intensity until its maximum (M_{MAX}), as there is no annihilation in the distal part of the motor axons (distal to the stimulation point; see Figure 8). A supramaximal stimulus intensity will discharge 100% of the efferent axons, yielding the M_{MAX} and blocking the generation of any H-reflex response due to the antidromic motor volley (see Figure 7).

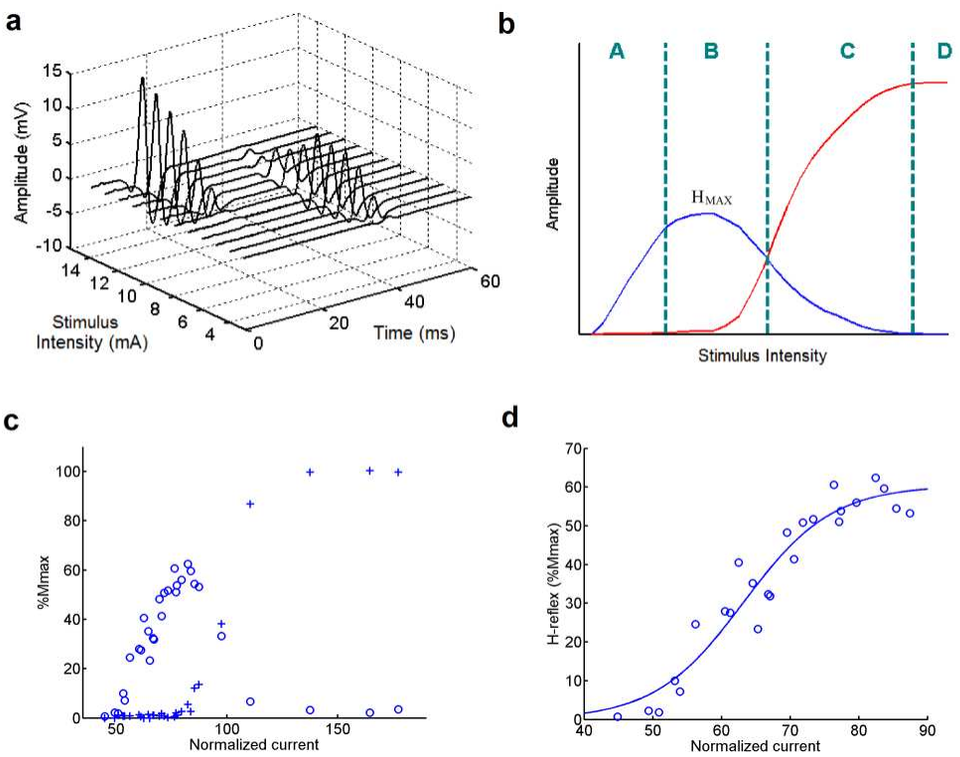

Figure 7. a) EMG traces recorded from the SO muscle showing changes in H-reflex and M-wave amplitudes as a function of stimulus intensity (unpublished data). Note the extinction of the H-reflex when the M_{MAX} is present in the recording (under the maximal stimulus intensity). **b)** Schematic recruitment curve with the peak-to-peak values of H-reflexes (blue) and M-waves (red) along the stimulus intensity. The regions A-D delimited by the green dashed vertical lines contain, respectively: the ascending limb of recruitment curve; motor threshold and H_{MAX}; descending limb of the curve; M_{MAX}. **c)** Recruitment curve obtained from the SO muscle of one representative subject. Data based on [10]. The circles and crosses represent the peak-to-peak amplitude values of the H-reflex and M-wave, respectively. **d)** Same data from **c** showing a sigmoidal fit to the ascending limb of the H-reflex recruitment curve. Data based on [9], but figures are unpublished.

http://dx.doi.org/10.5772/54870

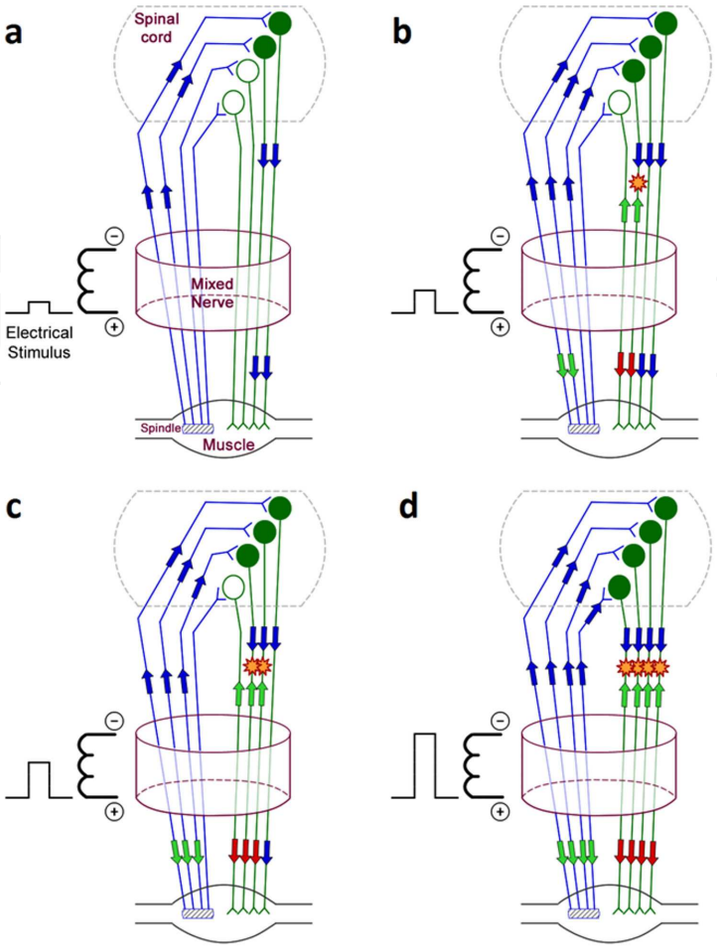

Figure 8. Schematics illustrating the recruitment of sensory and motor fibers by transcutaneous electrical stimulus. The stimulus intensity increases from **a** to **d** (see also the corresponding A-D regions in Figure 7) but the duration is always the same, 1ms. Note the bidirectional propagation of potentials (toward the spinal cord and muscle) in **b**-**d**. The blue arrows indicate the afferent volley (travelling across the blue axons) and the action potentials reflexively evoked in the motor axons (green cells) that will generate the H-reflex. The red arrows represent the orthodromic motor activation (see also Figure 6) that will generate the M-wave. The green arrows represent the antidromic volleys in either sensory or motor axons. The green arrows in the motor axons will cause a collision (indicated by a yellow star) with the reflexively evoked volley (blue arrows) in the efferent fibers. **a)** For low intensity stimulus the smallest MUs (filled circles) are recruited according to the size principle and no collision is observed. At this point only the H-reflex (without M-wave) is present in the EMG recording (see also Figure 7). **b)** With the increased intensity of electrical stimulation (1ms rectangular pulse), a few motor axons discharge action potentials that propagate antidromically leading to the annihilation of spikes. At this point the H-reflex is accompanied by an M-wave in the EMG recording. The M-wave has a shorter latency than the H-reflex because it is a direct response, i.e., it does not travel to the spinal cord and back to the muscle (red arrows reach the muscle before the blue ones). **c)** The stimulus intensity is much higher and the collision occurs in a larger number of efferent axons, despite the number of afferents recruited by the electrical stimulation being the same (or even higher) than in situation **b**. At this point the H-reflex amplitude is lower than the M-wave (C region of Figure 7b). **d)** The supramaximal intensity recruits 100% of the sensory and motor fibers inducing 100% of annihilation. No H-reflex is identified in the EMG recording and the M-wave reaches its maximal amplitude (M_{MAX}) (D region of Figure 7b).

In this scenario, the H-reflex will never reflect the activation of all the MNs within the pool, even if the stimulus intensity is increased. Instead, this reflex response reaches a maximum (H_{MAX}) as a result of a balance between mechanisms that tend to change the reflex amplitude

when the stimulus is increased. The main mechanism that increases H-reflex amplitude (assuming the subject is in a relaxed and controlled state) is the larger number of Ia axons activated by the higher intensity stimulus. The main mechanism that decreases the H-reflex amplitude in response to a stimulus intensity increase is the above mentioned collision of action potentials in the efferent axons. Other mechanisms that may also contribute to decrease the H-reflex amplitude for a higher stimulus amplitude include (1) the activation of Ib afferents (see schematic in Figure 6) [20], (2) the activation of large-diameter cutaneous afferents, (3) the firing of Renshaw cells in response to the synchronous antidromic (or orthodromic) firing of MNs in the pool [19, 23]. These longer latency mechanisms have their putative effect on H-reflex amplitude because the later phases of the H-reflex waveform (after its rise) have been associated with the longer latency oligosynaptic pathways that excite the MNs [18]. For stimulus intensities above that corresponding to H_{MAX} (from the beginning of the descending phase of the recruitment curve, Figure 7b and c), the larger the number of efferents undergoing collision the lower the amplitude of the H-reflex (see Figure 7 and Figure 8).

It is always recommended keeping the amplitude of the test H-reflex in the ascending limb of the recruitment curve, where there is no (or very few) collision in the motor axons. The best fit for the ascending limb of the curve is a sigmoid (Figure 7d) [24]. This fitting is important to define some parameters that can be extracted from the curve, such as slope, current threshold and H_{MAX} [10] (see ahead). It is also highly recommended using a test H-reflex amplitude within the range of 20-30%M_{MAX} [25] because at this amplitude reflexes are more responsive to conditioning.

4.1.2. H-reflex amplitude and ongoing EMG activity under different conditions

The H-reflex can be evoked in different conditions: at rest, during voluntary muscle contraction, in upright stance, during rhythmic movements of different limbs, during walking, running, and so on [1, 10, 26]. Usually, H-reflex evoked during contraction of the homonymous muscle shows higher amplitude compared to H-reflex evoked at rest [1, 21] (Figure 9). This happens because the MNs that were not fired by the afferent volley caused by the electrical stimulus might reach the firing threshold during contraction due to the summation of EPSPs generated by the activation of DTs. Figure 9 shows an example of H-reflex obtained at rest and during tonic voluntary isometric contraction of the SO muscle. When the level of voluntary contraction increases (more MUs are recruited), the size of the H-reflex increases in parallel [26]. Therefore, care should be taken when the objective is to study the modulation of the H-reflex during motor activity as its amplitude depends on the excitability of the MNs in the pool [21]. In practical terms, it is crucial to maintain a constant level of muscle activity throughout the experiment [1, 21].

During a sustained voluntary contraction there is a momentary silence in the muscle activity (silent period) following the H-reflex, as seen in the EMG recording of Figure 10. The silent period is mainly ascribed to the after-hyperpolarization (AHP) of the MNs after the synchronous reflex activation, since the EPSPs caused by descending commands cannot ellicit another spike in the MN during its refractory period (which is related to the AHP). After this period, the constant descending drive causes the MNs to reach the firing threshold almost at the same

http://dx.doi.org/10.5772/54870

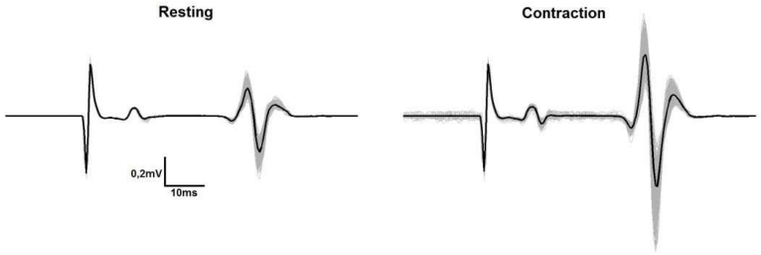

Figure 9. EMG recordings from the SO muscle showing the H-reflexes elicited in two different conditions, at rest and during isometric voluntary contraction (unpublished data). The black trace represents the averaged response.

time, i.e., when the refractory period ceases. This generates a rebound effect that can be seen in the EMG recordings of Figure 10. Other mechanisms might be involved in the generation of the silent period such as recurrent inhibition from Renshaw cells [27, 28]. This silent period has been shown to be useful, e.g. for the quantification of the degree of crosstalk between two muscles [14] and for the study of involuntary sustained muscle contraction after a train of stimuli [29].

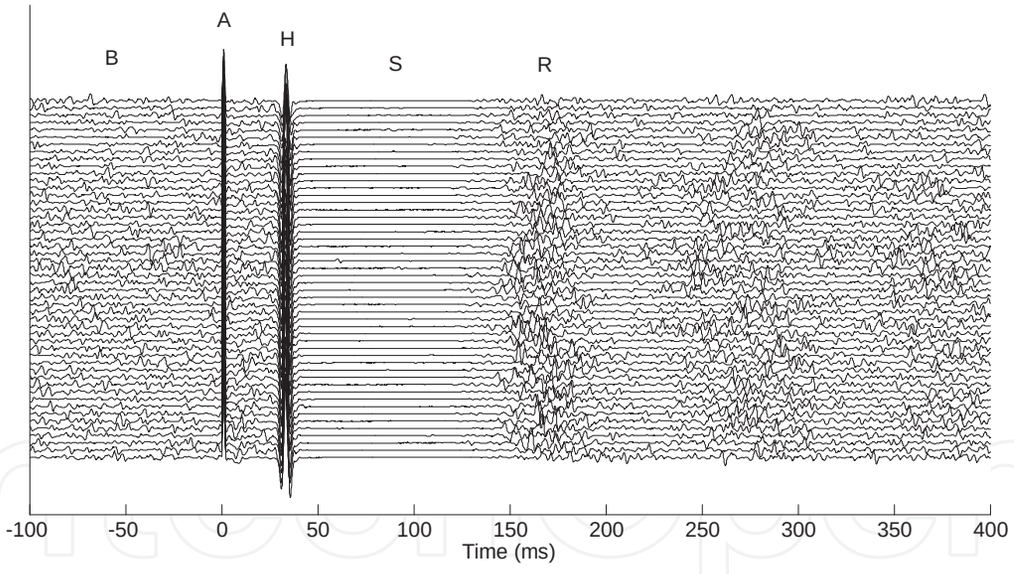

Figure 10. EMG recordings (unpublished data; *n* = 50) from the SO muscle during upright stance showing 100ms of background muscle activity (B) prior to the delivery of a stimulus to the PTN (A) to generate an H-reflex (H). Following the H-reflex, a clear silent period (S) of ~100ms is noticed. A rebound effect (R) can also be seen in the interval between 150 and 200ms.

Not only tonic voluntary contraction induces changes in reflex excitability. There are pre- and post-synaptic influences that affect H-reflex amplitude from a variety of sources. Presynaptic inhibition (PSI) is perhaps one of the most important mechanisms of reflex modulation [30]. By means of PSI the CNS can regulate the excitability of the stretch reflex pathway in different

motor contexts. For instance, it is generally accepted that PSI increases from the standing position to walking and even more during running [26].

Even in motor tasks involving rhythmic movements of limbs that mimic patterns of locomotor movements (e.g., arm swing during walking) modulation of reflex responses can be observed. It has been suggested that arm cycling in an ergometer decreases reflex amplitude of the SO muscle by increasing the level of PSI [31]. This result has been used as an evidence for the existence of a neuronal linkage between upper and lower limbs responsible for coordinated actions during locomotion [10]. An example of reduced amplitude H-reflex is shown in Figure 11.

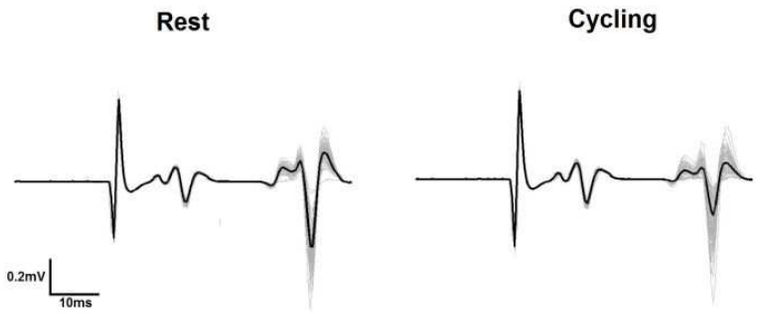

Figure 11. Comparison of H-reflex amplitude from the SO muscle at rest and during arm cycling. The constant amplit tude of the M-wave indicates that there were no changes in stimulus efficacy. The black trace represents the averaged response. Data based on [32], but figures are unpublished.

It is also possible to explore a wider range of MUs by examining the behavior of the H-reflex evoked at different stimulus intensities during the performance of a motor task. Therefore, instead of comparing test reflex responses of a given amplitude (just like those shown in Figure 11) that would represent a single point in the recruitment curve (hence, a limited fraction of active MUs within the pool), the whole recruitment curve can be analyzed (Figure 12). Several parameters may then be extracted from the recruitment curve and compared across conditions [10, 24] and the input-output relations of the system under study can be properly examined. Figure 12 shows an example of changes in the SO recruitment curve during rhythmic arm movements using a stepping ergometer. One can notice a reduction in H_{MAX} values as well as a right shifting of the curve, indicating changes in the threshold of reflex response (see the right panel of Figure 12). It is also possible to investigate changes in the recruitment gain by comparing the slope of the ascending curve between conditions. Note that no significant changes occurred in the M-wave curve (crosses), indicating that the stimulus efficacy was constant for both conditions.

In an attempt to better describe mechanisms responsible for reflex modulation, protocols based on conditioning stimulation have been developed. For example, it is possible to assess the level of PSI under different conditions [33, 34]. The technique (illustrated in Figure 13a) consists in applying a conditioning electrical stimulus to the CPN (1ms rectangular pulse) and a test stimulus to the PTN with a conditioning-to-test (CT) interval of 100ms [35] (compare gray and red traces in the upper panel of Figure 13b). The reflex response conditioned by the CPN

http://dx.doi.org/10.5772/54870

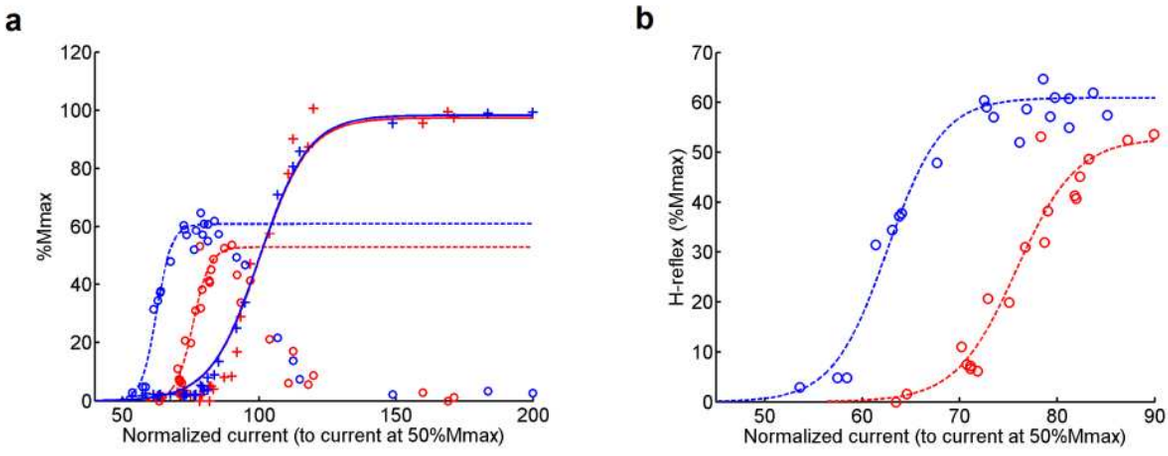

Figure 12. Recruitment curves obtained in two distinct conditions, at rest (blue) and during rhythmic arm movement (red). **a)** It is possible to note a decrease in H_{MAX} amplitude along with a right shift of the red curve. Note that the M-wave recruitment was very similar in both conditions. **b)** A closer inspection reveals a slight change in recruitment gain as indicated by the steeper slope of the blue curve compared to the red one. A clear change in H-reflex threshold can also be observed. Data based on [10], but figures are unpublished.

stimulus will have a lower amplitude as compared to the H-reflex elicited without conditioning due to the PSI effect. This procedure has been widely used in many research laboratories to investigate changes in the degree of PSI in different conditions.

Another pre-synaptic mechanism that affects H-reflex amplitude is post-activation depression (or homosynaptic depression - HD), which consists in a frequency-dependent reduction of reflex amplitude, i.e., when the stimuli are applied with frequencies higher than 0.1Hz (less than 10s interval) a depression in H-reflex amplitude is observed supposedly due to a reduced release of neurotransmitter in the Ia terminal [37, 38]. The HD is also exemplified in the upper panel of Figure 13b (green curve) that shows an averaged reflex response evoked at every 1s (1Hz stimulus frequency).

It is interesting to note a further decrease in H-reflex amplitude when both presynaptic mechanisms are present (PSI+HD; see the blue trace in Figure 13b). This result might be related to the increased frequency used for the conditioning stimulus (1Hz as compared to 0.1Hz used to obtain the trace in green) delivered 100ms before the test stimulus (also delivered at 1Hz to induce HD). Indeed, it was recently shown that an increased conditioning stimulus frequency enhances PSI of both H- [39] and T-reflexes [36].

4.2. The T-reflex

In section 4.1 we presented a technique for the assessment of stretch reflex excitability based on transcutaneous electrical stimulation (the H-reflex). Here we are going to discuss another way to investigate the same pathway by using a mechanical stimulus applied to the tendon in opposition to the electrical current applied to a peripheral mixed nerve. The target again will be the SO muscle. This technique has been used by clinicians to assess the integrity of the spinal

cord after injury or in neuropathologies [40]. Perhaps, the main concern about the use of this technique in scientific research is to maintain the mechanical stimulus consistent throughout the experiment. Several investigators have used an instrumented hammer [41, 42] designed to apply a somewhat controlled mechanical percussion to the tendon. An alternative approach is to use a powerful electromechanical shaker to achieve tendon mechanical stimulation [43]. The tip of the shaker is lightly pressed against the Achilles tendon to ensure reasonable stimulus reproducibility. The shaker can be controlled via software that provides the desired input waveform shape, amplitude and duration (e.g., a sinusoidal cycle with 10ms duration and excursion of ~3mm). An inbuilt accelerometer is a reliable alternative to provide a feedback from the shaker tip excursion and monitoring stimulus consistency [3, 43].

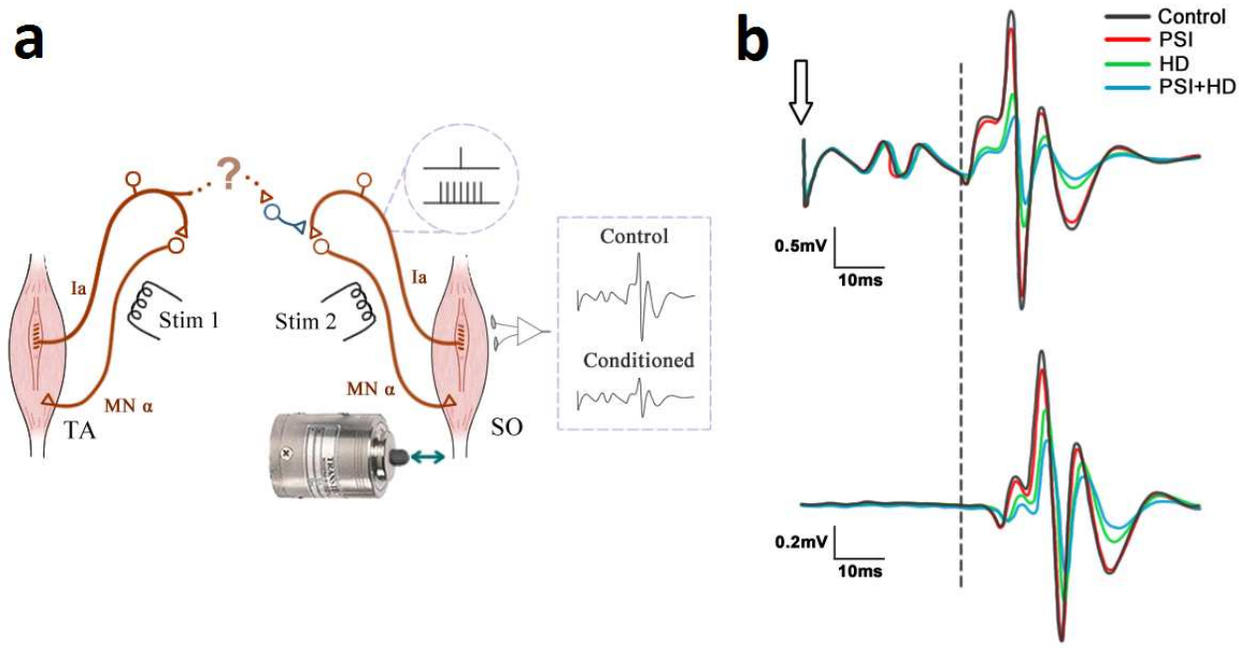

Figure 13. a) Schematic of the experimental setup for testing the presynaptic inhibition pathway. The test stimulus was either electrical (Stim2) or mechanical (indicated by the shaker in contact with the SO tendon). The interval between conditioning (Stim 1) and test stimuli (CT interval) was 100ms. SO afferent activation is shown in the dashed circle. For the H-reflex a single action potential is generated per Ia fiber, whereas the tendon stimulus evokes a burst of firing in Ia afferents. This difference might be responsible for the lesser sensitivity of the T-reflex to PSI as compared to the H-reflex (see text for details). **b)** Upper panel: Averaged H-reflex waveforms obtained in the SO muscle under different conditionings as compared to the control or no-conditioning case (in dark gray). The trace in red shows an H-reflex conditioned by a 1ms stimulus to the CPN to induce PSI on the afferent terminals of the SO muscle. The green trace represents the H-reflex under homosynaptic depression, HD (stimulus applied to the PTN at 1Hz). When the test and conditioned responses were obtained with interval of 1s (conditioned and test stimuli applied at 1Hz) an additional inhibition was observed (blue trace; HD+PSI). The vertical arrow shows the instant of stimulus delivery. Lower panel: the same as for upper panel showing the T-reflex. Note the longer delay as compared to the H-reflex (indicated by a horizontal dashed line). Results similar to those observed in H-reflex were attained for condition PSI+HD. Data based on [36], but figures are unpublished.

The main difference between both techniques (H and T reflexes) is that in the case of the H-reflex the stimulus bypasses the muscle spindles (it is applied directly to the nerve, see Figure 6). To generate the T-reflex the stimulus is applied distally, on the tendon of the muscle of

interest. The mechanical percussion induces a brief muscle stretch leading to the activation of spindle afferents. As a consequence, the mechanical stimulus generates a burst of firing in each afferent axon (mainly in Ia afferents). In contrast, the electrical stimulation produces only one spike per axon and at a more fixed latency (less sparse spikes arriving to the MN pool) than the burst due to the tendon tap [20] (see dashed circle in Figure 13). Therefore, the effect of asynchronous afferent bursts on the Ia-MN synapses will be different from a less dispersed volley of single action potentials. The MN depolarization (sum of EPSPs) generated by a more asynchronous afferent volley would produce a long rising time course in the membrane of the MN, giving time to other inputs (e.g., Ib afferents; see also Figure 6) mediated by oligosynaptic pathways to exert influence on the membrane of the postsynaptic cell [20]. Therefore, conditioning effects on T-reflex might be different from effects observed on H-reflex. For instance, T-reflex has been shown to be less responsive to a conditioning that induces PSI compared to the H-reflex [44] (see Figure 13). Despite the relatively lower sensitivity to PSI, the T-reflex also showed a stronger inhibitory effect when the conditioning stimulus was applied at higher frequency (1Hz), as for the H-reflex (see previous section) [36]. However, postsynaptic effects (e.g., mediated by RI) may have similar strength for both reflexes (see section 5.2.1; [44, 45]) regardless of the stimulus frequency.

Another important difference is related to the sensitivity of reflex responses to the fusimotor system excitability. T-reflexes are differentially susceptible to γ-MN activity (that regulates the muscle spindle sensitivity) as compared to H-reflexes [46]. All these aspects need to be taken into account in the interpretation of results and/or comparisons between both types of reflex responses.

4.3. The F-wave

F-waves are recorded routinely in clinical neurophysiological practice [47]. The F wave is a late response that occurs in a muscle following stimulation of its motor nerve, evoked by antidromic activation ("backfiring") of a fraction of the MNs. Typically, F-waves are evoked in response to a strong electrical stimulus (supramaximal stimulation) applied to a peripheral nerve. Action potentials traveling orthodromically reach the muscle fiber, thereby eliciting a strong M-response (M_{MAX}). The action potentials traveling antidromically (see arrows in Figure 6) reach the cell bodies of the MNs making a small fraction of them to fire. This causes orthodromic action potentials to travel back towards the muscle, generating a relatively small amplitude CMAP called F-wave. Several measurements can be done on the F responses, including peak-to-peak amplitude, duration, latency (period between stimulation and F-wave response), and persistency (number of F-waves obtained per number of stimulations). Most electrophysiologists agree that F-wave latency constitutes a valuable parameter that reflects conduction properties of motor axons, being even more reliable than distal motor conduction measurements used to detect mild or early generalized abnormalities [48]. Although the use of F waves for assessing MN excitability is controversial [49], they are sensitive to changes in MN excitability [48] and have been used to assess it in a variety of protocols [50, 51]. In contrast to the H-reflex, which is influenced by presynaptic effects (PSI and HD), the F response is not a reflex (is not elicited by Ia volley), hence its generation is related solely to the MN membrane

potential, which depends on the EPSPs and IPSPs the MN is receiving. Figure 14 shows F-wave recordings from the SO muscle (in response to supramaximal stimulation to the PTN) obtained in a subject at rest.

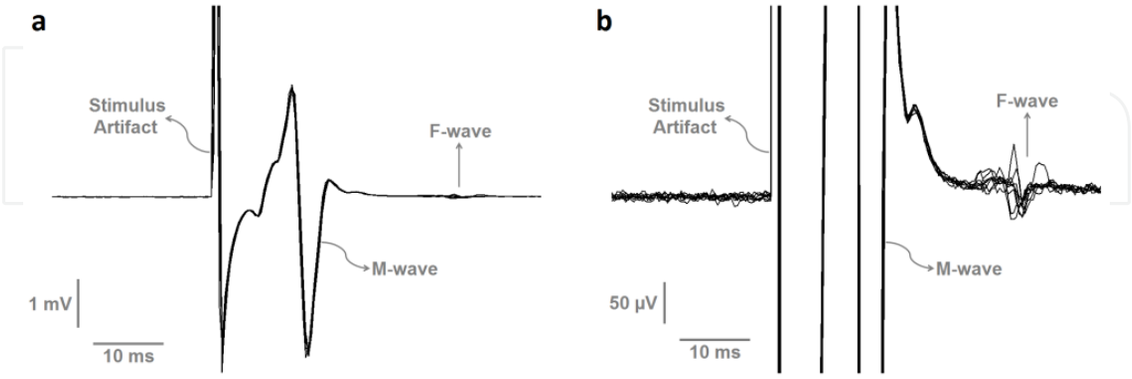

Figure 14. Nine superimposed EMG signals from the SO muscle showing stimulus artifacts, M-waves (M_{MAX}) and F-waves obtained in response to supramaximal stimulation (rectangular pulses with 0.2ms duration) delivered to the PTN of a resting subject (unpublished data). Surface stimulating electrodes were positioned with the cathode ($2cm^2$) on the popliteal fossa and the anode ($8cm^2$) on the patella. The stimulus intensity used to elicit F-waves was above that necessary to elicit M_{MAX}. The same recordings are shown in **a** and **b**, with different amplitude gains (note the calibration bars).

4.4. The V-wave

As described in section 4.1, when a supramaximal stimulus is delivered to the nerve of a relaxed muscle, an M-wave is observed in the EMG with short latency and no H-reflex is observed due to the collision (see Figure 8) between antidromic and orthodromic spikes (there could be F-waves, but they are not our focus here). However, if the subject maintains a steady voluntary contraction, and the same supramaximal stimulus is delivered to the peripheral nerve, a reflex response appears at a latency equal to the H-reflex. This reflex response, frequently referred to as a V-wave (associated with a voluntary drive), is an electrophysiological variant of the H-reflex and is used to measure the level of efferent drive [52-54].

The rationale behind the genesis of this response is that the descending drive activates a subset of MNs in the spinal cord making their axons conduct action potentials orthodromically. These action potentials collide with the antidromic volley generated at the electrical stimulation site by the supramaximal stimulus applied to the peripheral mixed nerve. Thus, this subset of MNs (recruited by the descending command) will be susceptible to be activated by the reflex afferent volley generated by the supramaximal electrical stimulus. Hence, the V-wave amplitude roughly reflects the number of spinal MNs being activated by the volitional drive, as well as the excitability associated with the stretch reflex pathway (previously discussed in section 4.1).

This electrophysiological measure has been used in several human neurophysiology studies, for instance: (1) neuronal plasticity associated with resistance training in healthy subjects [52]; (2) short-term effects of neuromuscular electrical stimulation [55]; (3) multiple sclerosis [56].

In the next section, we will present simulation results regarding the mechanisms behind the genesis of the V-wave.

5. Results from simulations

5.1. General description of the simulator

In this section, we will present simulation results that are valuable to better understand some mechanisms underlying the conditioning of muscle activity discussed previously in this chapter. The simulations were carried out in a multi-scale web-based neuromuscular simulator (dubbed ReMoto) that is freely accessible at http://remoto.leb.usp.br. A complete description of the simulator may be found elsewhere [4, 5]. Briefly, the simulator provides a detailed modeling of four spinal motor nuclei that command leg muscles responsible for ankle extension (SO; medial gastrocnemius - MG; lateral gastrocnemius - LG) and ankle flexion (TA). Each nucleus encompasses a MN pool and spinal INs mediating recurrent inhibition (by means of Renshaw cells), RI (by means of inhibitory Ia INs that receive inputs from antagonist muscles), and Ib inhibition. Individual spinal neurons are modeled following biophysical data from both cat MNs and INs, including active ionic channels responsible for the genesis of action potentials (sodium and fast potassium) and afterhyperpolarization (slow potassium). MN dendrites have an L-type calcium channel yielding a persistent inward current that is activated by the presence of neuromodulators in the spinal cord [57]. Ia and Ib afferents are present in ReMoto so as to allow studies on spinal reflexes (e.g., H-reflex) generated by electrical stimulation applied to a nerve (PTN for SO, LG and MG; CPN for TA). Model parameter values (e.g., axon conduction velocity, ionic channel time constants, maximum synaptic conductances) and default numbers of elements (i.e. spinal neurons and afferents) are based on experimental data from cats or humans. Some of the parameter values were adjusted so that the dynamic behavior of an individual model matches those experimentally observed in cats or humans, for example, MN frequency-current (*f-I*) curves, post-synaptic potentials time course, and IN discharge patterns.

The MN pool drives muscle units, which generate both electrical (MUAPs) and mechanical activity (force twitches). For each muscle, one output is the EMG, expressed as the sum of all MUAPs, and the other output is force, being the sum of the twitches of all muscle units. Muscle twitches are modeled as the impulse responses of second-order critically-damped systems [58]. MUAPs occurring at the muscle surface are modeled by first- and second-order Hermite-Rodriguez functions [59], which are randomly attributed to each MU. MUAP amplitude and durations are chosen to match intramuscular MUAPs recorded from humans. To model the MUAP recorded by bipolar surface electrodes at the muscle's surface, each intramuscular signal is re-scaled depending on the MU positioning within the muscle cross-section [60], thus representing the spatio-temporal filtering due to the volume conductor (see section 2.2). A white Gaussian noise is added to the resultant surface EMG and this signal is band-pass filtered to mimic a real EMG signal recorded in experiments.

Volitional muscle control is represented by the generation of random trains of action potentials in the DTs, which are modeled by independent nonhomogeneous renewal point processes with Gamma-distributed ISIs. The instantaneous firing rate or the ISI of these point processes can be modulated by mathematical functions (e.g., sinusoid and ramp) in order to generate dynamic motor behaviors, such as rhythmic muscle activity.

Recently, a detailed muscle spindle model was added to the simulator's structure, so that stretch reflex responses can be studied with the simulator [61]. This model (fully described in [62]) represents the nonlinear dynamics of three intrafusal muscle fibers (bag 1, bag 2 and chain). The combination of the fibers' tensions yields the instantaneous activity of the Ia and II afferents. Each intrafusal fiber has an active element, which represents the static and dynamic fusimotor activity coming from gamma MNs. A single muscle spindle model lies in parallel with each muscle model so that muscle stretch and stretch velocity modulate intrafusal fiber tension and consequently the afferent activity. Primary (Ia) and secondary (II) afferent activities are translated into spike trains that are transmitted to the spinal cord through an ensemble of peripheral nerve axons with an associated distribution of conduction velocities (type II afferents are at the moment available only in a downloadable version at the website). In order to represent the ISI variability observed in afferent axons [63], each spike train is represented by a non-homogeneous renewal point process with Gamma-distributed ISIs, whose intensity is modulated by the correspondent muscle spindle output (i.e., Ia or II). In addition, a linear recruitment of afferents is adopted so that during low afferent activity only a small fraction of afferents are discharging and the increase in afferent activity (from muscle spindle model) results in the recruitment of additional afferent axons.

5.1.1. Simulated H and T reflexes

H and T reflexes can be studied in ReMoto by activating (electrically or mechanically) the monosynaptic pathway encompassing Ia afferents, MN pool, and muscle (including the spindle). Oligosynaptic pathways [23] that may contribute to the H and T reflexes are not yet available in the simulator. Due to its multi-scale structure one may evaluate neurophysiological mechanisms and test hypotheses that are unfeasible with human experiments. Recent results [64] of conditioning effects on H and T reflexes are presented below, with emphasis on RI, which is an important inhibitory pathway associated with the control of movements [65, 66].

The friendly interface of ReMoto allows the easy set up of H- and T-reflex simulations using the structure depicted in Figure 15. The SO motor nucleus encompasses 900 type-specified MNs (800 S-type, 50 FR-type, and 50 FF-type), which receives synaptic contacts from Ia afferents (400 with 90% connectivity) of the PTN. In order to generate test H-reflexes, electrical stimuli (1ms rectangular pulses) are delivered at the nerve in a point equivalent to the popliteal fossa (0.66m from the spinal cord and 0.14m to the muscle end-plate). Figure 16a shows the M-wave and H-reflex generated by a 13mA stimulus without conditioning, as well as the discharge times of Ia afferents and MUs that were recruited directly by the electrical stimulus (early recruited MUs) and reflexively by Ia-to-MN excitation, respectively.

http://dx.doi.org/10.5772/54870

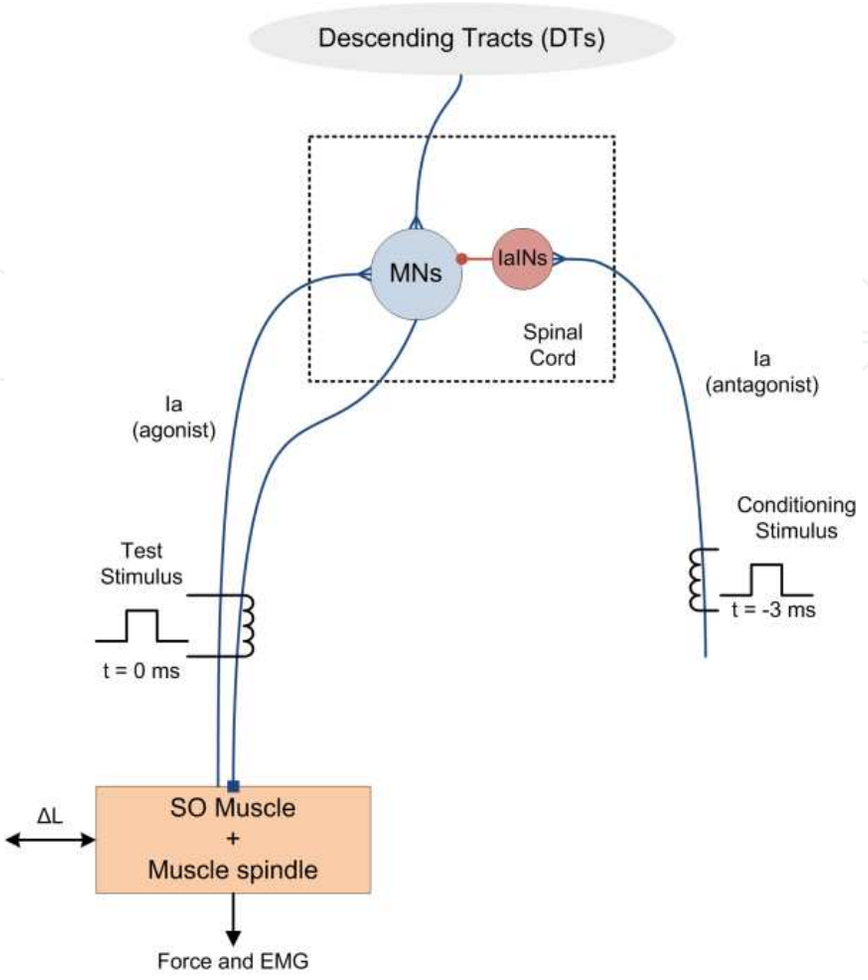

Figure 15. Schematic diagram of the neuromuscular system used to simulate H-reflex, T-reflex and V-wave of the SO muscle. An electrical pulse with appropriate amplitude delivered to the PTN elicits a direct M-wave and a test reflex (H-reflex), which can be observed in the simulated EMG. Similarly, the V-wave can be generated after a supramaximal stimulus delivered to the PTN during a sustained voluntary contraction evoked by the activity of DTs. Test T reflexes can be observed in the EMG after the application of an idealized SO muscle stretch (ΔL) that evokes a phasic response of muscle spindles and a burst of firing in Ia afferents. To simulate a conditioned H- or T-reflex due to RI, the antagonist CPN was stimulated with a CT interval equal to -3ms. For the T-reflex, an additional 7ms interval was added to account for the difference in reflex latencies.

Test T-reflexes can be simulated by applying an idealized stretch (10ms triangular-shaped stretch) to muscle fibers (see the schematic in Figure 15 and the time course in the lower panel of Figure 16b) in order to evoke a response in the muscle spindle model, which reflexively activates the spinal MNs by means of Ia afferents. The upper panel in Figure 16b shows the T-reflex generated with amplitude similar to the H-reflex described in the paragraph above (~25%M_{MAX}). It is worth noting that in these simulations a similar number of spinal MNs were recruited by the afferent volley evoked by the electrical (H-reflex) and mechanical stimulus (T-reflex), suggesting that despite the asynchronous discharge in Ia fibers during the T-reflex (see Ia afferent discharges in Figure 16b; [20]), the excitatory post-synaptic effect is similar between the electrically- and mechanically-evoked reflexes. A remarkable difference between these reflexes is the latency in which each wave is observed in the simulated EMG. The T-reflex

is shifted by approximately 7ms with respect to latency of the H-reflex, which represents the conduction time between the point of mechanical (muscle tendon) and electrical (popliteal fossa) stimulations [44, 45] (see also the vertical line in Figure 13b for experimental data).

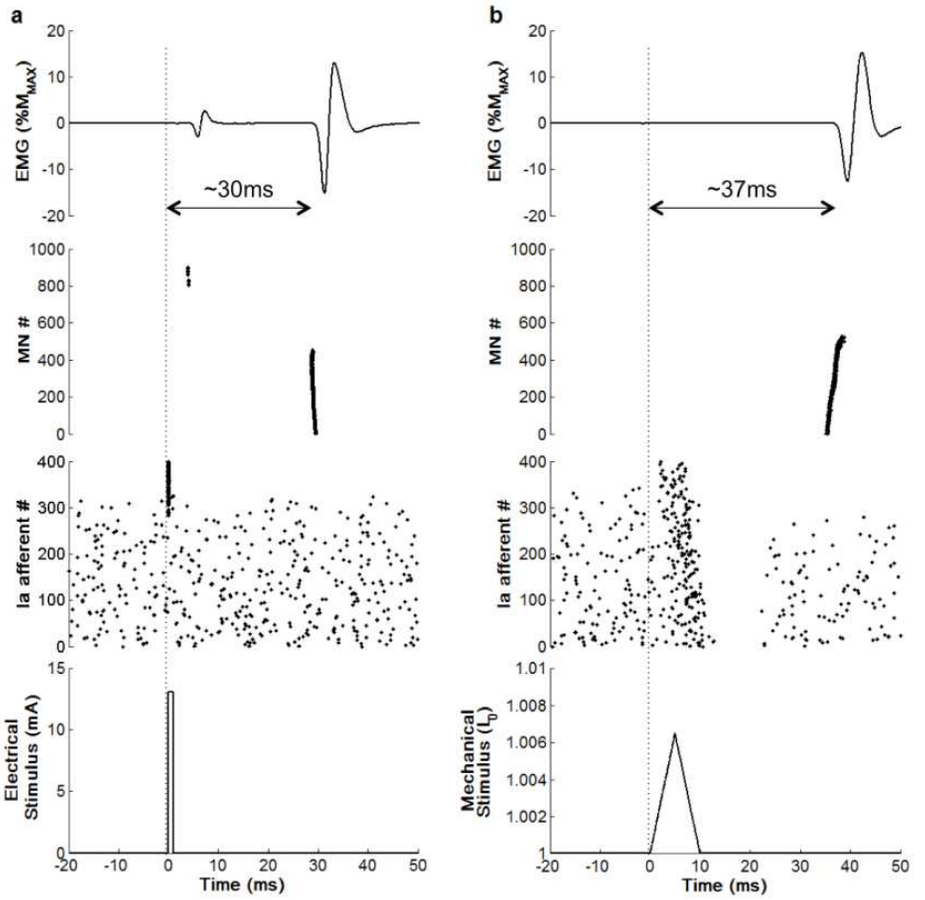

Figure 16. Simulated H and T reflexes (data based on [64], but figures are unpublished). **a)** From top to bottom: SO EMG showing the M-wave and the test H-reflex; raster plots of MU discharges at the muscle end-plate; raster plots of Ia afferent discharges at the popliteal fossa; and electrical stimulus delivered to the PTN at the popliteal fossa. **b)** From top to bottom: SO EMG showing the test T-reflex; raster plots of MU discharges at the muscle end-plate; raster plots of Ia afferent discharges at the popliteal fossa; and idealized mechanical stimulus (normalized to the optimal muscle length, L_0) delivered directly to the muscle spindle model. In both simulations, Ia afferents had a random low-frequency background discharge, which is compatible with the experimental data recorded from humans [63, 67]. Differences in latencies between the H- and T-reflex are due to the different places of stimulus application.

5.1.2. Conditioning effects from the activation of the reciprocal inhibition pathway

In this set of simulations, we have evaluated the conditioning effects of the RI pathway on the amplitude of H and T reflexes. Test reflexes were evoked as described in the preceding section; nevertheless, a conditioning stimulus was applied to the CPN, which innervates the antagonist muscle (see schematic in Figure 15), in order to elicit an afferent volley to the inhibitory Ia INs (IaINs) that make inhibitory synapses on the SO MN pool. The stimulus amplitude (1ms duration) delivered to the CPN was 1.1MT (i.e. 10% above the MT). In addition, the connec-

http://dx.doi.org/10.5772/54870

tivity between Ia afferents and IaINs was set at 100%, while a 20% connectivity was adopted in the IaINs-to-MNs pathway. Similarly to experimental studies, a CT interval equal to -3ms was adopted for the H-reflex simulations (i.e. the conditioning stimulus was delivered 3ms before the test stimulus). To account for the difference in reflex latencies, 7ms was added to the CT interval in T-reflex simulations [44, 45].

Top panels in Figure 17 (a and b) show the EMGs of the SO muscle for a control condition (red curves) and when a conditioning stimulus was applied to the CPN (black curves). RI reduced the H-reflex amplitude by ~40% of its control value (Figure 17a), whereas the amount of inhibition observed in T-reflex was ~53% of its control value (Figure 17b). This difference was not statistically significant (*t*-Student test; $p > 0.05$; $n = 5$), supporting the hypothesis that the post-synaptic effect is similar in both H and T reflexes [45].

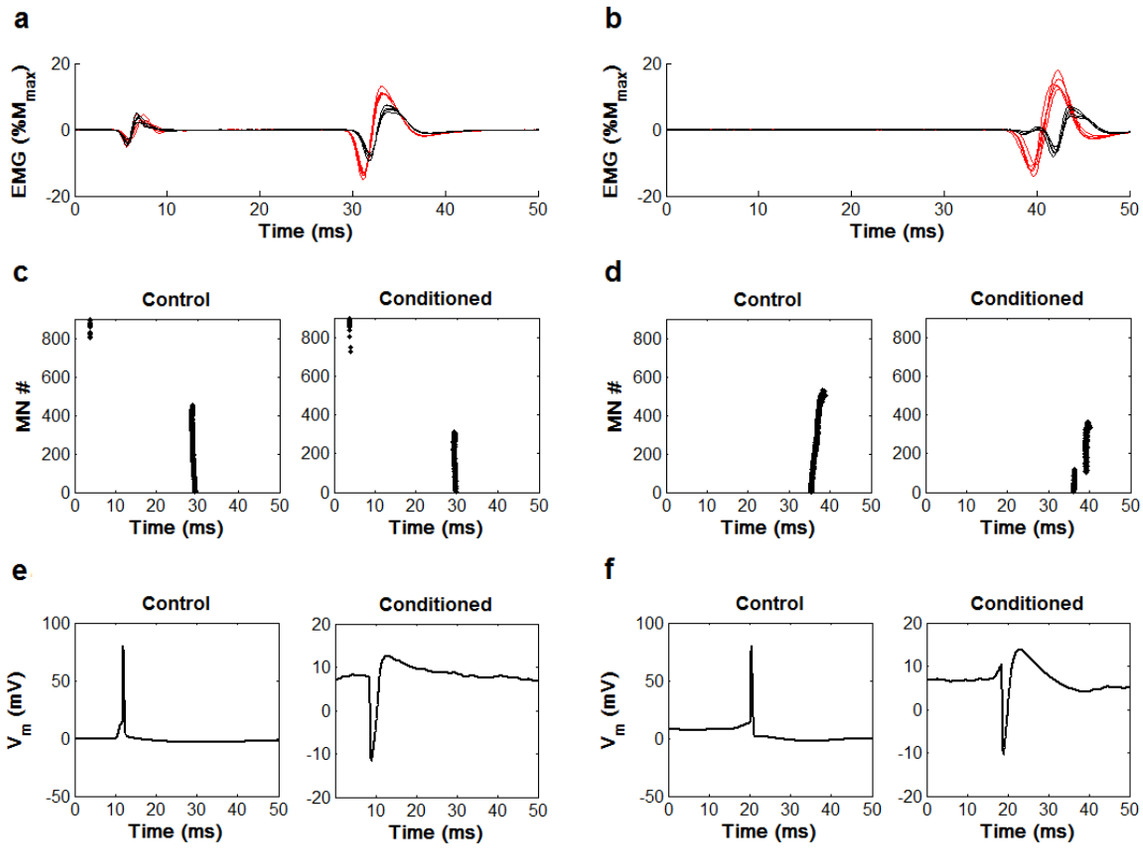

Figure 17. Conditioning effects of the reciprocal inhibition (RI) on H and T reflexes. Data based on [64], but figures are unpublished. **a)** Simulated SO EMGs showing M waves and the H reflexes evoked with (black curves) and without (red curves) a conditioning stimulus delivered to the CPN (five repetitions for each condition). **b)** The same as **a** but for T reflexes. **c)** Raster plots of MU discharges at the muscle end-plate for a single simulation of H-reflex in a control condition (left-side graph) and with a conditioning stimulus delivered to the CPN (right-side graph). **d)** The same as **c** but for a single simulation of T-reflex. **e)** Membrane potential time course of a single MN during a H-reflex simulation. The left-side graph shows an action potential generated in a control condition, whereas the right-side graph shows the post-synaptic potentials observed when a conditioning stimulus is delivered to the CPN. **f)** The same as **e** but for a single MN during a T-reflex simulation. The zero in all displayed abscissas indicates the moment when the stimulus (either electrical or mechanical) was delivered.

Approximately the same number of spinal MNs was de-recruited by the RI in both reflexes (see Figure 17c and d), with a more pronounced effect on high-threshold neurons. This finding (which is readily accessible in the simulator, but not in human experiments) can be explained by the higher input conductance of these cells, which yield smaller compound excitatory post-synaptic potentials (EPSP). Hence, these cells will be operating near their firing thresholds, which means that they will be more easily de-recruited by the arrival of small IPSPs (see right-side graphs in Figure 17e and f). Another result that is unique to the simulations is the recording of intracellular membrane potentials. In the lower panels of Figure 17 (e and f), the membrane potential of a single MN is shown. In a control condition (i.e. without conditioning), this MN is recruited by both electrically- and mechanically-evoked synaptic volleys (left-side graphs). Similarly, the arrival of an IPSP is effective in de-recruiting this MN in both reflexes (right-side graphs), suggesting that RI has a similar effect on these responses. In addition, the compound EPSP observed in the MN soma has a similar time course for both reflexes, reinforcing the hypothesis that post-synaptic effects are similar between H- and T-reflexes [45].

5.2. Simulated V-wave

As described in section 4.4, the V-wave is believed to reflect the level of the efferent drive maintained by a voluntary command. To test this hypothesis, we have used the neuromuscular simulator described above to generate V waves in the SO muscle [68]. The structure depicted in Figure 15 (with exception of the conditioning stimulus) was also used in this simulation, with the MN pool encompassing 900 type-identified MNs and 100 independent axons representing the DTs. The spike train associated to each DT axon was modeled as Poisson point processes with a given mean intensity and the connectivity between DTs and the MN pool was fixed at 30%. At time 1s, a supramaximal electrical stimulus was delivered to the PTN evoking an M_{MAX} and subsequently a V-wave. Changes in V-wave amplitude (normalized with respect to the M_{MAX}) were evaluated by changes in the mean ISI of DTs, mimicking the neuronal plasticity that is supposed to occur after training [52, 55, 56].

Figure 18 shows the simulated SO EMG (upper panels) for two different intensities of the descending drive (mean ISI equal to 3.8ms in Figure 18a and 3ms in Figure 18b), which were chosen to match the ratio V/M_{MAX} observed in the literature [52]. The increase in the ratio reflects the increase in the number of active MNs (from 233 to 426; see lower panels in Figure 18), which roughly corresponded to the number of MNs discharging before the electrical stimulation. This information cannot be accessed in human experiments, emphasizing, therefore, the relevance of mathematical modeling and computer simulations.

The reader can notice that the background EMG activity before the stimulus delivery is slightly different between the two simulated conditions. However, the interference pattern is more susceptible to nonlinear summation and cancellation of MUAPs. Therefore, the V-wave may be a more reproducible and reliable measure of the efferent drive, which can increase or decrease due to different factors, e.g, neuronal plasticity following training and hyper-excitability of spinal MNs following neurological diseases, such as stroke and amyotrophic lateral sclerosis [54, 56].

http://dx.doi.org/10.5772/54870

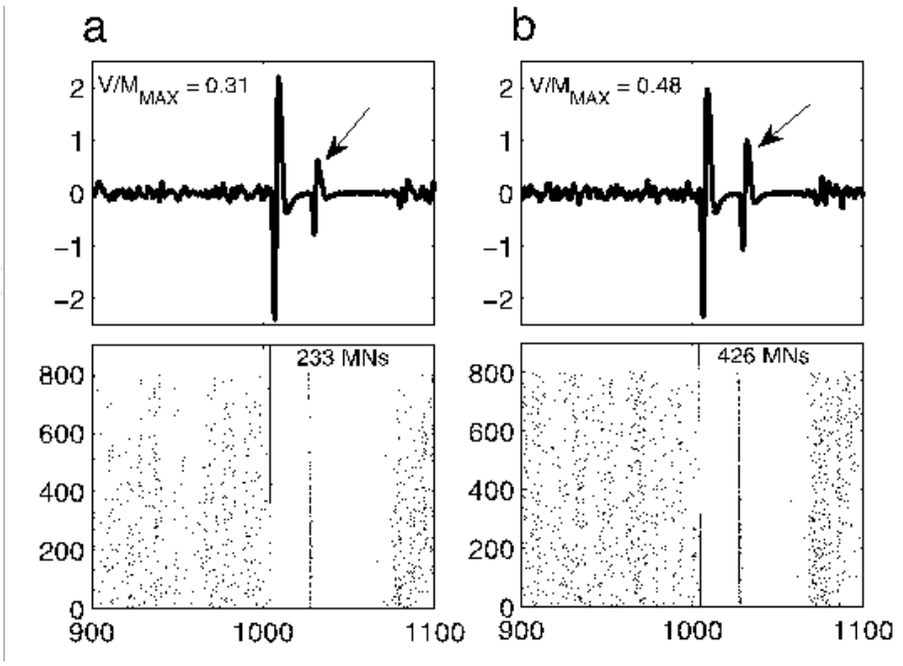

Figure 18. V-waves (arrows) preceded by M-waves in ReMoto simulation of SO EMG (upper panels). Raster plots of MN spikes (lower panels). **a)** Lower-intensity descending drive. **b)** Higher intensity descending drive. Data based on [68].

6. Conclusion

In this chapter we have discussed several aspects regarding the use of surface EMG in a variety of human neurophysiology protocols. Different conditioning effects on the interference pattern and phasic responses, which can be used to infer spinal cord mechanisms, were presented and discussed. Finally, in order to refine the understanding of some underlying mechanisms involved in motor control, as well as to facilitate the interpretation of EMG data, we have introduced a comprehensive web-based simulator of the neuromuscular system with open-access and a friendly interface. The simulation results can be used to test hypothesis raised from the analysis of experimental data and to propose new questions to be addressed in different experimental protocols. The techniques and models presented here might be useful for researchers/clinicians who intend to conduct experiments on both healthy subjects and patients with neuromuscular disorders.

Acknowledgements

The authors are grateful to CNPq (Brazilian Science Foundation), FAPESP (São Paulo Research Foundation) and Canadian Bureau for International Education (PDRF Program) for their financial support.

Author details

Rinaldo André Mezzarane, Leonardo Abdala Elias, Fernando Henrique Magalhães, Vitor Martins Chaud and André Fabio Kohn

Biomedical Engineering Laboratory, University of São Paulo, São Paulo, Brazil

References

[1] Pierrot-Deseilligny E, Burke D. The circuitry of the human spinal cord: Spinal and corticospinal mechanisms of movement. Cambridge: Cambridge University Press; 2012.

[2] Hultborn H, Meunier S, Morin C, Pierrot-Deseilligny E. Assessing changes in presynaptic inhibition of Ia fibres: a study in man and the cat. Journal of Physiology. 1987;389:729-56.

[3] Mezzarane RA, Kohn AF, Couto-Roldan E, Martinez L, Flores A, Manjarrez E. Absence of effects of contralateral group I muscle afferents on presynaptic inhibition of Ia terminals in humans and cats. Journal of Neurophysiology. 2012;108:1176-85.

[4] Cisi RRL, Kohn AF. Simulation system of spinal cord motor nuclei and associated nerves and muscles, in a Web-based architecture. Journal of Computational Neuroscience. 2008;25(3):520-42.

[5] Elias LA, Chaud VM, Kohn AF. Models of passive and active dendrite motoneuron pools and their differences in muscle force control. Journal of Computational Neuroscience. 2012;33(3):515-31.

[6] Merletti R, Parker PA. Electromyography: physiology, engineering, and noninvasive applications. Hoboken: Wiley; 2004.

[7] De Luca CJ. Electromyography. In: Webster JG, editor. Encyclopedia of medical devices and instrumentation. New York: John Wiley & Sons; 2006. p. 98-109.

[8] Kandel ER, Schwartz JH, Jessell TM, Siegelbaum SA, Hudspeth AJ. Principles of neural science. 5 ed. New York: McGraw-Hill; 2013.

[9] De Luca CJ, Adam A, Wotiz R, Gilmore LD, Nawab SH. Decomposition of surface EMG signals. Journal of Neurophysiology. 2006;96(3):1646-57.

[10] Mezzarane RA, Klimstra M, Lewis A, Hundza SR, Zehr EP. Interlimb coupling from the arms to legs is differentially specified for populations of motor units comprising the compound H-reflex during "reduced" human locomotion. Experimental Brain Research. 2011;208:157-68.

[11] DeLuca CJ. The use of surface electromyography in biomechanics. Journal of Applied Biomechanics. 1997;13(2):135-63.

[12] Dumitru, D. Electrodiagnostic Medicine. Philadelphia: Hanley & Belfus; 1995

[13] Merletti R, Knaflitz M, DeLuca CJ. Electrically evoked myoelectric signals. Critical Reviews in Biomedical Engineering. 1992;19(4):293-340.

[14] Mezzarane RA, Kohn AF. A method to estimate EMG crosstalk between two muscles based on the silent period following an H-reflex. Medical Engineering & Physics. 2009;31(10):1331-6.

[15] Capaday C, Cody FW, Stein RB. Reciprocal inhibition of soleus motor output in humans during walking and voluntary tonic activity. Journal of Neurophysiology. 1990;64:607-16.

[16] Petersen N, Morita H, Nielsen J. Evaluation of reciprocal inhibition of the soleus H-reflex during tonic plantar flexion in man. Journal of Neuroscience Methods. 1998;84:1-8.

[17] Magladery JW, McDougal DB, Jr. Electrophysiological studies of nerve and reflex activity in normal man. I. Identification of certain reflexes in the electromyogram and the conduction velocity of peripheral nerve fibres. Johns Hopkins Medicine Journal. 1950;86:265-90.

[18] Burke D, Gandevia SC, McKeon B. Monosynaptic and oligosynaptic contributions to human ankle jerk and H-reflex. Journal of Neurophysiology. 1984;52(3):435-48.

[19] Knikou M. The H-reflex as a probe: pathways and pitfalls. Journal of Neuroscience Methods. 2008;171(1):1-12.

[20] Burke D, Gandevia SC, McKeon B. The afferent volleys responsible for spinal proprioceptive reflexes in man. Journal of Physiology. 1983;339:535-52.

[21] Schieppati M. The Hoffmann reflex: a means of assessing spinal reflex excitability and its descending control in man. Progress in Neurobiology. 1987;28:345-76.

[22] Henneman E, Mendell LM. Functional organization of motoneuron pool and its inputs. Handbook of Physiology The nervous System. Bethesda (MD): American Physiological Society; 1982. p. 423-507.

[23] Misiaszek JE. The H-reflex as a tool in neurophysiology: its limitations and uses in understanding nervous system function. Muscle & Nerve. 2003;28(2):144-60.

[24] Klimstra M, Zehr EP. A sigmoid function is the best fit for the ascending limb of the Hoffmann reflex recruitment curve. Experimental Brain Research. 2008;186(1):93-105.

[25] Crone C, Hultborn H, Mazieres L, Morin C, Nielsen J, Pierrot-Deseilligny E. Sensitivity of monosynaptic test reflexes to facilitation and inhibition as a function of the test reflex size: a study in man and the cat. Experimental Brain Research. 1990;81:35-45.

[26] Stein RB, Capaday C. The modulation of human reflex during functional motor tasks. Trends in Neurosciences. 1988;11:328-32.

[27] Ashby P. Some Spinal Mechanisms of Negative Motor Phenomena in Humans. Negative Motor Phenomena. 1995;67:305-20.

[28] Mcnamara DC, Crane PF, Mccall WD, Ash MM. Duration of Electromyographic Silent Period Following Jaw-Jerk Reflex in Human Subjects. Journal of Dental Research. 1977;56(6):660-4.

[29] Nozaki D, Kawashima N, Aramaki Y, Akai M, Nakazawa K, Nakajima Y, et al. Sustained muscle contractions maintained by autonomous neuronal activity within the human spinal cord. Journal of Neurophysiology. 2003;90(4):2090-7.

[30] Rudomin P, Schmidt RF. Presynaptic inhibition in the vertebrate spinal cord revisited. Experimental Brain Research. 1999;129(1):1-37.

[31] Frigon A, Collins DF, Zehr EP. Effect of rhythmic arm movement on reflexes in the legs: Modulation of soleus H-reflexes and somatosensory conditioning. Journal of Neurophysiology. 2004;91(4):1516-23.

[32] Mezzarane RA, Zehr EP. Locomotor-related descending regulation and voluntary motor output interact to modulate H-reflex variability in leg muscles. 39th Annual Meeting of the Society for Neuroscience; 2009; Chicago.

[33] Faist M, Dietz V, PierrotDeseilligny E. Modulation, probably presynaptic in origin, of monosynaptic Ia excitation during human gait. Experimental Brain Research. 1996;109(3):441-9.

[34] Mezzarane RA, Kohn AF. Control of upright stance over inclined surfaces. Experimental Brain Research. 2007;180(2):377-88.

[35] Iles JF. Evidence for cutaneous and corticospinal modulations of presynaptic inhibition of Ia afferents from the human lower limb. Journal of Physiology. 1996;491:197-207.

[36] Mezzarane RA, Magalhães FH, Chaud VM, Elias LA, Kohn AF. Responsiveness of H- and T-reflexes of soleus muscle to presynaptic inhibition induced by a low frequency train of stimuli. 42nd Annual Meeting of the Society for Neuroscience; 2012; New Orleans.

[37] Hultborn H, Illert M, Nielsen J, Paul A, Ballegaard M, Wiese H. On the mechanism of the post-activation depression of the H-reflex in human subjects. Experimental Brain Research. 1996;108(3):450-62.

[38] Kohn AF, Floeter MK, Hallett M. Presynaptic inhibition compared with homosynaptic depression as an explanation for soleus H-reflex depression in humans. Experimental Brain Research. 1997;116(2):375-80.

[39] Roche N, Achache V, Lackmy A, Pradat-Diehl P, Lamy JC, Katz R. Effects of afferent stimulation rate on inhibitory spinal pathways in hemiplegic spastic patients. Clinical Neurophysiology. 2012;123(7):1391-402.

[40] Mezzarane RA, Nakajima T, Zehr EP. Modulation of soleus stretch reflex amplitude during rhythmic arm cycling movement after stroke. 41st Annual Meeting of the Society for Neuroscience; 2011; Washington.

[41] Archambeault M, de Bruin H, McComas A, Fu W. Tendon reflexes elicited using a computer controlled linear motor tendon hammer. 2006 28th Annual International Conference of the IEEE Engineering in Medicine and Biology Society, Vols 1-15. 2006:2342-5.

[42] Chung SG, Van Rey E, Bai ZQ, Rymer WZ, Roth EJ, Zhang LQ. Separate quantification of reflex and nonreflex components of spastic hypertonia in chronic hemiparesis. Archives of Physical Medicine and Rehabilitation. 2008;89(4):700-10.

[43] Fornari MCD, Kohn AF. High frequency tendon reflexes in the human soleus muscle. Neuroscience Letters. 2008;440(2):193-6.

[44] Morita H, Petersen N, Christensen LO, Sinkjaer T, Nielsen J. Sensitivity of H-reflexes and stretch reflexes to presynaptic inhibition in humans. Journal of Neurophysiology. 1998;80(2):610-20.

[45] Enriquez-Denton M, Morita H, Christensen LO, Petersen N, Sinkjaer T, Nielsen JB. Interaction between peripheral afferent activity and presynaptic inhibition of ia afferents in the cat. Journal of Neurophysiology. 2002;88(4):1664-74.

[46] Rossi-Durand C. The influence of increased muscle spindle sensitivity on Achilles tendon jerk and H-reflex in relaxed human subjects. Somatosensory and Motor Research. 2002;19(4):286-95.

[47] Daube JR, Rubin DI. Clinical Neurophysiology. 3rd ed. Oxford: Oxford University Press; 2009.

[48] Panayiotopoulos CP, Chroni E. F-waves in clinical neurophysiology: a review, methodological issues and overall value in peripheral neuropathies. Electroencephalography and Clinical Neurophysiology. 1996;101(5):365-74.

[49] Espiritu MG, Lin CS, Burke D. Motoneuron excitability and the F wave. Muscle & Nerve. 2003;27(6):720-7.

[50] Magalhaes FH, Kohn AF. Vibration-induced extra torque during electrically-evoked contractions of the human calf muscles. Journal of NeuroEngineering and Rehabilitation. 2010;7:26.

[51] Salih F, Steinheimer S, Grosse P. Excitability and recruitment patterns of spinal motoneurons in human sleep as assessed by F-wave recordings. Experimental Brain Research. 2011;213(1):1-8.

[52] Aagaard P, Simonsen EB, Andersen JL, Magnusson P, Dyhre-Poulsen P. Neural adaptation to resistance training: changes in evoked V-wave and H-reflex responses. Journal of Applied Physiology. 2002;92(6):2309-18.

[53] Pensini M, Martin A. Effect of voluntary contraction intensity on the H-reflex and V-wave responses. Neuroscience Letters. 2004;367(3):369-74.

[54] Solstad GM, Fimland MS, Helgerud J, Iversen VM, Hoff J. Test-retest reliability of v-wave responses in the soleus and gastrocnemius medialis. Journal of Clinical Neurophysiology. 2011;28(2):217-21.

[55] Gondin J, Duclay J, Martin A. Soleus- and gastrocnemii-evoked V-wave responses increase after neuromuscular electrical stimulation training. Journal of Neurophysiology. 2006;95(6):3328-35.

[56] Fimland MS, Helgerud J, Gruber M, Leivseth G, Hoff J. Enhanced neural drive after maximal strength training in multiple sclerosis patients. European Journal of Applied Physiology. 2010;110(2):435-43.

[57] Elias LA, Kohn AF. Individual and collective properties of computationally efficient motoneuron models of types S and F with active dendrites. Neurocomputing. 2013;99:521-33.

[58] Milner-Brown HS, Stein RB, Yemm R. The contractile properties of human motor units during voluntary isometric contractions. Journal of Physiology. 1973;228(2): 285-306.

[59] Lo Conte LR, Merletti R, Sandri GV. Hermite expansions of compact support waveforms: applications to myoelectric signals. Ieee Transactions on Biomedical Engineering. 1994;41(12):1147-59.

[60] Fuglevand AJ, Winter DA, Patla AE, Stashuk D. Detection of motor unit action-potentials with surface electrodes - Influence of electrode size and spacing. Biological Cybernetics. 1992;67(2):143-53.

[61] Chaud VM, Elias LA, Watanabe RN, Kohn AF. A simulation study of the effects of activation-dependent muscle stiffness on proprioceptive feedback and short-latency reflex. 4th IEEE RAS/EMBS International Conference on Biomedical Robotics and Biomechatronics; Rome: IEEE; 2012. p. 133-8.

[62] Mileusnic MP, Brown IE, Lan N, Loeb GE. Mathematical models of proprioceptors. I. Control and transduction in the muscle spindle. Journal of Neurophysiology. 2006;96(4):1772-88.

[63] Matthews PB, Stein RB. Regularity of primary and secondary muscle spindle afferent discharges. Journal of Physiology. 1969;202(1):59-82.

[64] Elias LA, Chaud VM, Magalhaes FH, Mezzarane RA, Kohn AF. H and T reflexes evaluated by a biologically-realistic neuromuscular model. 42nd Annual Meeting of the Society for Neuroscience; 2012; New Orleans.

[65] Hyngstrom AS, Johnson MD, Miller JF, Heckman CJ. Intrinsic electrical properties of spinal motoneurons vary with joint angle. Nature Neuroscience. 2007;10(3):363-9.

[66] Di Giulio I, Maganaris CN, Baltzopoulos V, Loram ID. The proprioceptive and agonist roles of gastrocnemius, soleus and tibialis anterior muscles in maintaining human upright posture. The Journal of Physiology. 2009;587(Pt 10):2399-416.

[67] Aniss AM, Diener HC, Hore J, Gandevia SC, Burke D. Behavior of human muscle receptors when reliant on proprioceptive feedback during standing. Journal of Neurophysiology. 1990;64(2):661-70.

[68] Elias LA, Chaud VM, Watanabe RN, Kohn AF. Application of a web-based simulator to a study of neuromuscular training in humans. BMES 2011 Annual Meeting; 2011; Hartford.

IntechOpen